WALAILAK JOURNAL
http://wjst.wu.ac.th Engineering and Physical Sciences

Steady Free Convection and Mass Transfer MHD Flow of a Micropolar Fluid in a Vertical Channel with Heat Source and Chemical Reaction

Manoj Kumar NAYAK[1], Gouranga Charan DASH[2] and Lambodar Prased SINGH[3]

[1]*Department of Physics, Radhakrishna Institute of Technology and Engineering, Biju Patnaik University of Technology, Odisha, India*
[2]*Department of Mathematics, Institute of Technical Education and Research, Siksha 'O' Anusandhan University, Odisha, India*
[3]*Department of Physics, Utkal University, Odisha, India*

([*]Corresponding author's e-mail: mnkec1973@gmail.com)

Received: 13 August 2014, Revised: 26 October 2014, Accepted: 25 December 2014

Abstract

This paper reports a numerical study of steady free convection and mass transfer flow of a conducting micropolar fluid between two vertical walls in the presence of temperature dependent heat source/sink and chemical reaction under the influence of a transverse magnetic field. The numerical solution of the governing differential equations are obtained by using a fourth-order Runge-Kutta method along with the shooting technique for a wide range of emerging parameters. A striking result is to note that microrotation is independent of the material property and vortex viscosity in the middle layers of the channel. The conformity of the findings of the present study is in good agreement with the results reported earlier in the absence of mass transfer associated with a chemical reaction.

Keywords: Free convection, micropolar fluid, heat-source/sink, chemical reaction, magnetic field

Nomenclature

B	material parameter	C_p	specific heat at constant pressure
C	non-dimensional species parameter	C_0	reference species concentration
D	diffusion coefficient, m^2/s.	g	acceleration due to gravity
H_0	uniform transverse magnetic field, *Tesla*	j	micro-inertial density
k	kinematic rotational viscosity, $N.s/m^2$	K_c	chemical reaction parameter
L	distance between two vertical walls	m	temperature ratio parameter
M	magnetic parameter	m_1	concentration ratio parameter
R	vortex viscosity parameter	S	heat source/sink parameter
T	non-dimensional temperature	t	non-dimensional time, s
T_0	reference temperature	u	non-dimensional velocity, m/s.
ω	micro-rotation velocity		

Greek letters

α thermal diffusivity, m^2/s.
γ local buoyancy parameter
μ kinematic viscosity, $N.s/m^2$
ρ density of the fluid

Introduction

Micropolar fluids proposed by Eringen [1] simulate accurately the flow characteristics of polymeric additives, geomorphological sediments, colloidal and haematological suspensions, liquid crystals, lubricants etc. Studies of the flows of heat convection in micropolar fluids focus mainly on flat surfaces by Rahman *et al*. [2-6]. Hassanien *et al*. [7] have considered natural convection flow of micropolar fluid along a vertical and a permeable semi-infinite plate embedded in a porous medium. The problem of fully developed natural convection heat and mass transfer of a micropolar fluid between porous vertical plates with asymmetric wall temperatures and concentrations is analyzed by Abdulaziz and Hashim [8]. Desseaux and Kelson [9] have studied the flow of a micropolar fluid bounded by a stretching sheet. Mitarai *et al*. [10] have presented the effect of collisional granular flow as a micropolar fluid. El-Arabawy [11] has shown the effect of suction/injection on the flow of a micropolar fluid past a continuously moving plate in the presence of radiation. Aydin and Pop [12,13] observed natural convection in a heated enclosure filled with a micropolar fluid. The unsteady natural convection heat transfer of a micropolar fluid over a vertical surface with constant heat flux was studied by Damseh *et al*. [14]. Chamkha *et al*. [15] analyzed numerical and analytical solutions of the developing laminar free convection of a micropolar fluid in a vertical parallel plate channel with asymmetric heating.

Parida *et al*. [16] have studied magnetohydrodynamic (MHD) heat and mass transfer in a rotating system with periodic suction. Recently, Zucco *et al*. [17] discussed magneto-micropolar fluid over a stretching surface embedded in a Darcian porous medium by the numerical network method. Further, Eldabe *et al*. [18] reported their work on hydromagnetic peristaltic flow on micropolar biviscosity fluid. Another interesting work related to MHD viscoelastic flow with heat and mass transfer was reported very recently by Kar *et al*. [19]. Helmy *et al*. [20] studied MHD free convection flow of a micropolar fluid past a vertical porous plate.

Flow of fluids with internal heat sources / sinks are of great practical as well as theoretical interest. The fluid motion develops slowly following the development of non-uniformity in the temperature field. The volumetric heat generation / absorption term exerts strong influence on the flow and heat transfer when the temperature difference is appreciably large. The analysis of temperature field as modified by the heat source / sink in a moving fluid is important in view of chemical reactions and problems concerned with dissociating fluids. Acharya *et al*. [21] studied the flow problems in the presence of a heat source. Foraboschi *et al*. [22] have assumed 2 state volumetric heat generation as depending on temperature difference.

$$\theta = \begin{cases} \theta_0(T - T_0), & T \geq T_0 \\ 0, & T < T_0 \end{cases} \tag{1}$$

In many chemical engineering processes chemical reactions take place between a foreign mass and the working fluid which moves due to stretching or otherwise of a surface. A chemical reaction is said to be first order and homogenous if its rate of reaction is directly proportional to the concentration and it occurs as a single phase volume reaction. Muthucumaraswamy [23] studied the effects of a chemical reaction on a moving isothermal vertical surface with suction and Afify [24] considered MHD free convection flow and mass transfer over a stretching sheet with chemical reaction.

The purpose of the present study is to develop a mathematical model of a conducting micropolar fluid flow, heat and mass transfer in a vertical channel in the presence of a transverse magnetic field. The heat transfer associated with internal temperature dependent volumetric heat source/sink as well as concentration distribution accompanied by the chemical reaction of the reactive species obeying a first order reaction subject to a resistive force of electromagnetic origin is the main theme of the modelling. The novelty of the present work is to study the effects of magnetic field, species concentration and chemical reaction over and above other physical parameters on the velocity and microrotation. The numerical solutions are obtained and analyzed to bring out the effects of various emerging parameters.

The present investigation is likely to have a bearing in geothermal areas where flow of chemically treated ground water or industrial fluid exhibiting micropolar fluid properties occurs. Further, the application of a transverse magnetic field fixed to the body should reduce the heat transfer at the stagnation point and increase the body's drag. Both these results are desirable for protecting a vehicle reentering the atmosphere as studied by Cramer and Pai [25].

Mathematical formulation

Consider steady laminar free convective MHD flow of a conducting micropolar fluid between 2 vertical walls subject to a transversely applied magnetic field such that the induced electric current due to the motion of the fluid does not distort the applied magnetic field. This assumption is true if the magnetic Reynolds number of the flow is very small, which is the case in many aerodynamic applications where rather low velocities and electrical conductivities are involved. This is always the case for electrically conducting liquid metals.

The vertical walls are separated by a distance L and having temperatures T_1' and T_2' and concentrations C_1' and C_2'. The x'- axis is taken along one of the vertical walls while y'- axis is normal to it (**Figure 1**). The walls are assumed to be infinitely long so that the dependent variables are independent of the vertical co-ordinate. For free convection, let us consider a vertical channel with walls maintained at different temperatures and concentrations in a still micropolar fluid. The velocity of the fluid is induced by heat and mass transfer from the plates and it is small. Hence, the dissipation due to the viscosity is neglected in this problem but body forces due to gravity are added following Pai [26]. The micropolar fluid may be considered as an incompressible fluid if the temperature and concentration gradients are not large. Under these assumptions the governing equations corresponding to the considered model are derived as follows;

$$(\mu + k)\frac{d^2u'}{dy'^2} + k\frac{d\omega'}{dy'} + \rho g\frac{T' - T_0'}{T_0'} + \rho g\frac{C' - C_0'}{C_0'} - \sigma H_0^2 u = 0 \tag{2}$$

$$\gamma\frac{d^2\omega'}{dy'^2} - k(2\omega' + \frac{du'}{dy'}) = 0 \tag{3}$$

$$\alpha\frac{d^2T'}{dy'^2} + S'(T' - T_0') = 0 \tag{4}$$

$$D\frac{d^2C'}{dy'^2} + K_c'(C' - C_0') = 0 \tag{5}$$

where $\gamma = \left(\mu + 0.5k\right) j$, $\alpha = \dfrac{k}{\rho C_p}$ (6)

The boundary conditions are;

$$\left.\begin{aligned} u' = 0, \omega' = -\frac{1}{2}\frac{du'}{dy'}, T' = T_1', C' = C_1' \quad at\ y' = 0 \\ u' = 0, \omega' = -\frac{1}{2}\frac{du'}{dy'}, T' = T_2', C' = C_2' \quad at\ y' = L \end{aligned}\right\} \tag{7}$$

In the energy equation the heat due to viscous dissipation is neglected for small velocities. Soret-Dufour (thermal diffusion and diffusion-thermo) effects are also ignored in the diffusion equations which is true when the species concentration level is very low.

Introducing the following non-dimensional quantities;

$$\left.\begin{aligned} & y = y'/L,\ \omega = \frac{\omega'\mu}{\rho g L}, u = \frac{u'\mu}{\rho g L^2}, M^2 = \frac{\sigma H_0^2 L^2}{\mu}, \\ & T = \frac{T' - T_0'}{T_0'}, C = \frac{C' - C_0'}{C_0'}, m = \frac{T_2' - T_0'}{T_0'}, m_1 = \frac{C_2' - C_0'}{C_0'} \\ & B = L^2/j, S = S'L^2/\alpha, K_c = K_c' L^2/D, R = k/\mu \end{aligned}\right\} \tag{8}$$

the Eqs. (2) - (5) reduce to;

$$\left(1 + R\right)\frac{d^2u}{dy^2} + R\frac{d\omega}{dy} - M^2 u = -T - C \tag{9}$$

$$\left(1 + \frac{R}{2}\right)\frac{d^2\omega}{dy^2} - BR(2\omega + \frac{du}{dy}) = 0 \tag{10}$$

$$\frac{d^2T}{dy^2} + ST = 0 \tag{11}$$

$$\frac{d^2C}{dy^2} + K_c C = 0 \tag{12}$$

and the corresponding boundary conditions (7) become;

$$\left.\begin{aligned} u=0, \omega=-\frac{1}{2}\frac{du}{dy}, T=1, C=1 \quad at\ y=0 \\ u=0, \omega=-\frac{1}{2}\frac{du}{dy}, T=m, C=m_1 \quad at\ y=1 \end{aligned}\right\} \tag{13}$$

Numerical solution

The governing equations are solved numerically by applying the fourth order Runge-Kutta method along with the shooting technique. This method has been proven to be appropriate and gives accurate results for boundary layer equations. In the present calculations, the value of y is taken as 1 and grid size or step size of y is taken as $\Delta y = 0.001$ and the convergence criterion is set to 10^{-5} for better consideration of the boundary conditions. The solutions are obtained for the dimensionless velocity, microrotation, temperature and concentration and shown graphically.

Let $u = y_1, u' = y_2$, $\omega = y_3$, $\omega' = y_4, T = y_5$, $T' = y_6$, $C = y_7$ and $C' = y_8$. (14)

so that $y_2' = \frac{1}{1+R}\left[M^2 y_1 - R\, y_4 - y_5 - y_7\right]$, (15)

$$y_4' = \frac{1}{1+R/2}\left[BR\left(2y_3 + y_2\right)\right], \tag{16}$$

$$y_6' = -Sy_5 \tag{17}$$

and $$y_8' = -K_c y_7 \tag{18}$$

with $y_a(1) = 0$, $y_b(1) = 0$, $y_a(3) = -0.5 y_a(2)$, $y_b(3) = -0.5 y_b(2)$, $y_a(5) = 1$, $y_b(5) = m$, $y_a(7) = 1$ and $y_b(7) = m_1$. (19)

Results and discussion

The governing equations for the problem of steady free convection and mass transfer flow of a micropolar fluid between 2 vertical walls in the presence of heat source/sink and chemical reaction are solved numerically by the Runge-Kutta method with a shooting technique which are represented for different values of governing parameters and the results are presented through graphs and tables.

From a practical point of view, it is important to know the effects of mass transfer, heat transfer and chemical reaction parameter of the reacting species on the flow field. For the purpose of calculation we have considered two cases (i) under symmetric distribution of temperature and concentration ($m = m_1 = 1$) i.e., $T_2' = 2T_0'$ and $C_2' = 2C_0'$ which correspond to the temperature and concentration at the plate $y = 1$ are twice the reference temperature and concentration. Moreover, $T = 1$ and $C = 1$, boundary conditions, correspond to $T_1' = 2T_0'$ and $C_1' = 2C_0'$. Hence, the results are pertaining to the case of equal temperature and concentration (ii) asymmetric distribution ($m = m_1 = 0$) corresponds to unequal temperature and concentration at the plates.

The parabolic velocity distribution bears a common characteristic i.e. the presence of a heat source and exothermic reaction ($S > 0, K_c > 0$) escalates the velocity at all points in comparison with the case of

a sink and endothermic reaction $(S<0, K_c<0)$ overriding the effects of other parameters on the flow phenomena for both symmetric and asymmetric temperature and concentration distribution.

The velocity distribution is almost symmetrical about the middle of the channel with a crest at $y=0.5$ (approx.). The above distribution is a common phenomenon reported in literature and in particular by Ravi *et al*. [27]. They have considered the micropolar fluid flow in a vertical channel in the absence of mass transfer associated with a chemical reaction.

Moreover, from Eqs. (9) and (10), it is evident that the vortex viscosity parameter *R* attributes micropolar properties, and even enjoys more priority than the material parameter *B*. If *R* = 0 both the governing equations reduce to;

$$\frac{d^2u}{dy^2}=-T-C, \tag{20}$$

$$\frac{d^2\omega}{dy^2}=0 \tag{21}$$

which indicate that the effect of the material parameter automatically becomes ineffective.

Figure 2 (asymmetric case : $m=m_1=0$) exhibits the velocity profiles for different values of the vortex viscosity parameter *R*, the heat source/sink parameter *S*, the material parameter *B* and chemical reaction parameter K_c for both the source and exothermic reaction $(S>0, K_c>0)$ as well as the sink and endothermic reaction $(S<0, K_c<0)$. It is observed that an increase in *S* and K_c increases velocity whereas an increase in *R,* decreases it in the presence of a source and exothermic reaction as well as a sink and endothermic reaction. But increase in *B* causes a decrease in velocity in the presence of source and exothermic reaction whereas opposite effect is observed in the presence of sink and endothermic reaction.

Figure 3 (symmetric case : $m=m_1=1$) presents the velocity profiles with different values of *R*, *S*, *B* and K_c for both $S>0, K_c>0$ and $S<0, K_c<0$. The effects of all the parameters qualitatively remain same as that of asymmetric case besides the symmetricity of the profiles.

From **Figures 4** and **5**, it is remarked that the effect of the Lorentz force due to the interaction of the magnetic field with conducting micropolar fluid resists the motion of the flow as a result of which the value of the velocity decreases in both $m=m_1=0$ and $m=m_1=1$.

Figures 6 and **7** display the velocity profiles for asymmetric and symmetric distribution of temperature and concentration. It is interesting to note that the change in the material parameter does not affect the profiles in the absence of a heat source and chemical reaction but the vortex viscosity $R\left(=\frac{k}{\mu}\right)$ reduces the velocity substantially. This observation is in good agreement with Ravi *et al*. [27]. Thus, it is inferred that the kinematic rotational viscosity resists the flow producing a thinner hydrodynamic boundary layer.

Figure 8 presents the micro rotation profiles for asymmetric distribution of temperature and concentration in the presence of a source/sink and for both types of reactions. One of the striking features of the variation is that the middle layers of the profiles remain unaffected due to variation of pertinent parameters governing the flow. This phenomena is an outcome of the reverse rotation of the layers beyond the middle of the channel. Another feature is to note that the presence of a sink under the influence of an endothermic reaction attains higher values of $|\omega|$ in the lower half of the channel than the presence of the source with an exothermic reaction. It is also evident that micro-rotation assumes negative

values in the lower half whereas positive values are found in the upper half. As regards the effects of individual parameters, it is clear that an increase in absolute values of heat sink and endothermic reaction, $|\omega|$ increases whereas the opposite effect is observed in case of the material parameter *B*. A decrease in micro-rotation for higher values of *B* was also observed by Ravi *et al*. [27]. Further it is concluded that opposite flow behavior is exhibited in the upper half of the channel with respect to material property for $S > 0, K_c > 0$.

Figure 9 exhibits the case of symmetric distribution. One interesting feature of micro-rotation is that both the categories of profiles ($S > 0, K_c > 0 \& S < 0, K_c < 0$) have a common point of intersection at the middle of the channel whereas in the asymmetric case this is not so. Other features of the profile remain the same as that of the asymmetric case.

Figure 10 shows that an increase in the magnetic parameter (M) decreases the microrotation (ω) in the layers $y \geq 0.5$ and the opposite effect is observed in the other half of the channel in the asymmetric case. **Figure 11** depicts that the effect of *M* in the symmetric case remains the same as that of the asymmetric case. However, higher microrotation is experienced in the symmetric case.

One important observation from **Figures 12** and **13** is that the effect of the material property of the micropolar fluid on the micro-rotation is not significant in the absence of a source and chemical reaction which is evident from the curves IV and V. It is further observed that an increase in the vortex viscosity parameter decelerates $|\omega|$ while other features remain the same.

Figure 14 provides a graphical representation of the temperature variation for the source or sink and two values of temperature ($m = 0$ and 1). Eq. (11) is a linear equation and the corresponding boundary conditions indicate that temperature variation is controlled by the source and temperature parameter. **Figure 14** also shows that the temperature increases at all points when *S* varies from −1 to 3. For $S = 0$, Eq. (11) reduces to $\frac{d^2T}{dy^2} = 0$ and hence the temperature varies linearly. It is interesting to note that temperature at the upper plate characterizes the thermal boundary layer. In the present case when $m = 1$, the distribution is almost symmetrical and parabolic but when $m = 0$, the sharp fall in temperature is marked. Since the temperature at the lower plate is fixed at 1.0, the temperature at the upper plate matters for creating a thermal gradient and hence the thinning and thickening of the thermal boundary layer.

The variation of concentration is similar to that of temperature as the source/sink is replaced by the first order exothermic/endothermic reaction as shown in **Figure 15**.

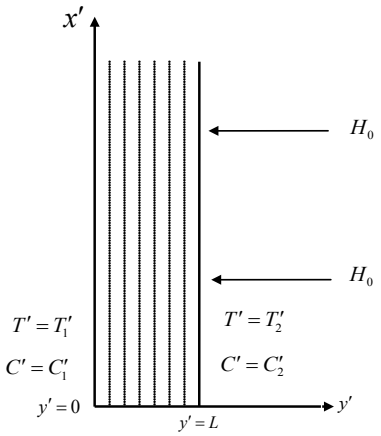

Figure 1 Schematic diagram of the flow model.

Table 1 shows the maximum values of *u* in an asymmetric case ($m = m_1 = 0$). The velocity attains a maximum increase from 0.09967 to 0.16187 by 38.43 % for $S > 0, K_c > 0$ while it increases from 0.05934 to 0.09401 by 36.88 % for $S < 0, K_c < 0$.

Table 2 shows variation of u_{max} with respect to variation of R, S, B, K_c for $S > 0, K_c > 0$ and $S < 0, K_c < 0$ in an asymmetric case.

Table 3 shows the maximum values of *u* in a symmetric case ($m = m_1 = 1$). The velocity attains a maximum increase from 0.19769 to 0.29302 by 32.53 % at $y = 0.5$ for $S > 0, K_c > 0$ and 0.12055 to 0.17075 by 29.4 % at $y = 0.5$ for $S < 0, K_c < 0$.

Table 4 shows variation of u_{max} with respect to variation of R, S, B, K_c for S > 0, K_c > 0 and S < 0, K_c< 0 in a symmetric case.

Table 1 The magnitude of u_{max} with respect to *y* for $S > 0, K_c > 0$ and $S < 0, K_c < 0$ in an asymmetric case.

Source & Exothermic; Sink & Endothermic	**Distance (y)**	u_{max}	**Graphical representation**	**Maximum increase of u_{max} (%)**
Source & Exothermic ($S > 0, K_c > 0$)	0.46	0.09967	Curve V	38.43
	0.45	0.11118	Curve VI	
	0.44	0.12413	Curve III	
	0.44	0.12895	Curve I	
	0.45	0.14099	Curve II	
	0.46	0.16187	Curve IV	
Sink & Endothermic ($S < 0, K_c < 0$)	0.45	0.05934	Curve V	36.88
	0.44	0.07935	Curve IV	
	0.43	0.08317	Curve II	
	0.43	0.08589	Curve I	
	0.44	0.08741	Curve III	
	0.45	0.09401	Curve VI	

Table 2 Variation of u_{max} with respect to variation of R, S, B, K_c for $S > 0, K_c > 0$ and $S < 0, K_c < 0$ in an asymmetric case.

Source & Exothermic; Sink & Endothermic	**Physical Parameters**	**Graphical representation**	u_{max}
Source & Exothermic ($S > 0$, $K_c > 0$)	$0.5 \le R \le 1.5$	Curve II & Curve V	$0.09967 \le u_{\max} \le 0.14099$
	$1.0 \le S \le 2.0$	Curve II & Curve IV	$0.14099 \le u_{\max} \le 0.16187$
	$0.5 \le B \le 1.0$	Curve II & Curve III	$0.12413 \le u_{\max} \le 0.14099$
	$0.7 \le K_c \le 3.0$	Curve VI & Curve I	$0.11118 \le u_{\max} \le 0.12895$
Sink & Endothermic ($S < 0$, $K_c < 0$)	$0.5 \le R \le 1.5$	Curve II & Curve V	$0.05934 \le u_{\max} \le 0.08317$
	$-2.0 \le S \le -1.0$	Curve IV & Curve II	$0.07935 \le u_{\max} \le 0.08317$
	$0.5 \le B \le 1.0$	Curve II & Curve III	$0.08317 \le u_{\max} \le 0.08741$
	$-3.0 \le K_c \le -0.7$	Curve VI & Curve I	$0.08589 \le u_{\max} \le 0.0901$

Table 3 The magnitude of u_{max} with respect to *y* for $S > 0$, $K_c > 0$ and $S < 0$, $K_c < 0$ in a symmetric case.

Source & Exothermic; Sink & Endothermic	**Distance (y)**	u_{max}	**Graphical representation**	**Maximum increase of u_{max} (%)**
Source & Exothermic $(S > 0, K_c > 0)$	y = 0.5	0.19769	Curve V	32.53
		0.21878	Curve VI	
		0.24493	Curve III	
		0.25461	Curve I	
		0.27896	Curve II	
		0.29302	Curve IV	
Sink & Endothermic $(S < 0, K_c < 0)$		0.12055	Curve V	29.4
		0.15458	Curve IV	
		0.16218	Curve II	
		0.16767	Curve I	
		0.16978	Curve III	
		0.17075	Curve VI	

Table 4 Variation of u_{max} with respect to variation of R, S, B, K_c for S > 0, K_c > 0 and S < 0, K_c< 0 in a symmetric case.

Source & Exothermic; Sink & Endothermic	**Physical Parameters**	**Graphical representation**	u_{max}
Source & Exothermic $(S>0, K_c>0)$	$0.5 \le R \le 1.5$	Curve II & Curve V	$0.19769 \le u_{\max} \le 0.27896$
	$1.0 \le S \le 2.0$	Curve II & Curve IV	$0.27896 \le u_{\max} \le 0.29302$
	$0.5 \le B \le 1.0$	Curve II & Curve III	$0.24493 \le u_{\max} \le 0.27896$
	$0.7 \le K_c \le 3.0$	Curve VI & Curve I	$0.21878 \le u_{\max} \le 0.25461$
Sink & Endothermic $(S<0, K_c<0)$	$0.5 \le R \le 1.5$	Curve II & Curve V	$0.11655 \le u_{\max} \le 0.16218$
	$-2.0 \le S \le -1.0$	Curve IV & Curve II	$0.15458 \le u_{\max} \le 0.16218$
	$0.5 \le B \le 1.0$	Curve II & Curve III	$0.16218 \le u_{\max} \le 0.17075$
	$-3.0 \le K_c \le -0.7$	Curve VI & Curve I	$0.16767 \le u_{\max} \le 0.17075$

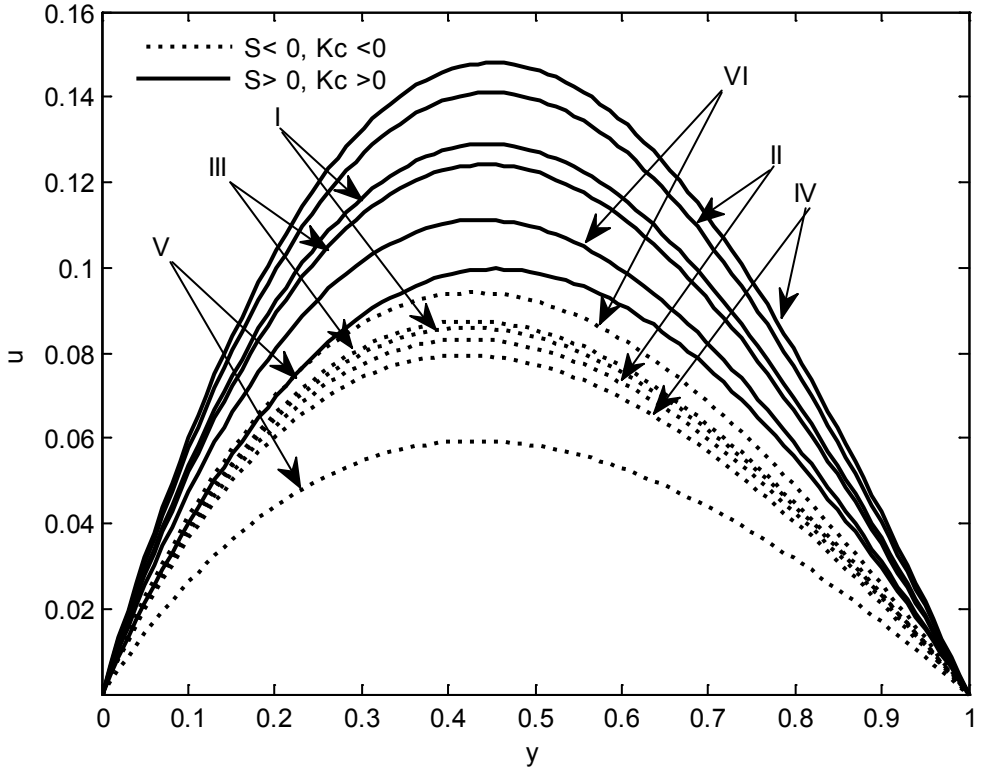

Curve	R	S	B	Kc	Curve	R	S	B	Kc
I	0.5	1.0	0.5	3.0	I	0.5	-1.0	0.5	-3.0
II	0.5	1.0	0.5	4.0	II	0.5	-1.0	0.5	-4.0
III	0.5	1.0	1.0	4.0	III	0.5	-1.0	1.0	-4.0
IV	0.5	2.0	0.5	4.0	IV	0.5	-2.0	0.5	-4.0
V	1.5	1.0	0.5	4.0	V	1.5	-1.0	0.5	-4.0
VI	0.5	1.0	0.5	0.7	VI	0.5	-1.0	0.5	-0.7

Figure 2 Velocity profiles showing the effects of R, S, B, K_c for M = 0 and $m = m_1 = 0$.

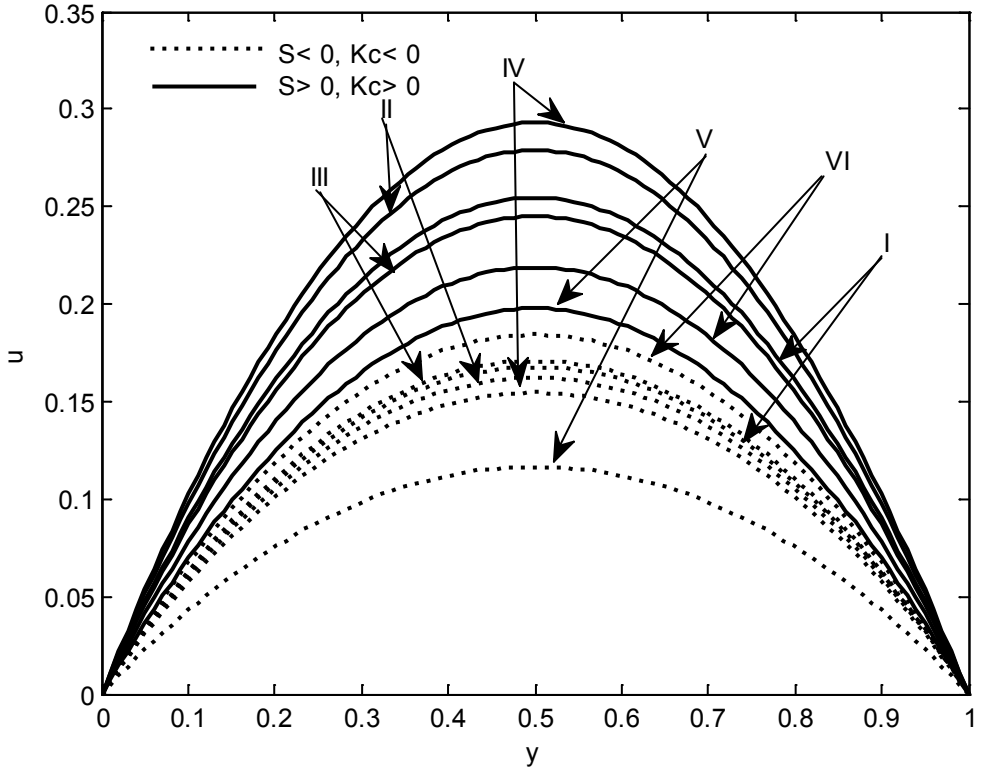

Curve	R	S	B	Kc	Curve	R	S	B	Kc
I	0.5	1.0	0.5	3.0	I	0.5	-1.0	0.5	-3.0
II	0.5	1.0	0.5	4.0	II	0.5	-1.0	0.5	-4.0
III	0.5	1.0	1.0	4.0	III	0.5	-1.0	1.0	-4.0
IV	0.5	2.0	0.5	4.0	IV	0.5	-2.0	0.5	-4.0
V	1.5	1.0	0.5	4.0	V	1.5	-1.0	0.5	-4.0
VI	0.5	1.0	0.5	0.7	VI	0.5	-1.0	0.5	-0.7

Figure 3 Velocity profiles showing the effects of R, S, B, K_c for M = 0 and $m = m_1 = 1$.

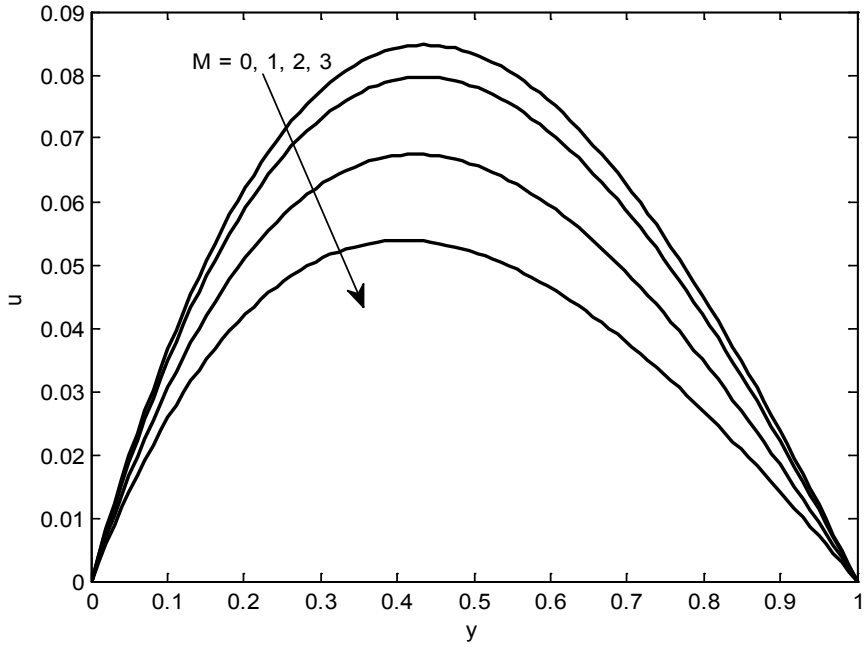

Figure 4 Velocity profiles showing the effects of *M* with $R = 0.5, S = 1.0, B = 0.5$ and $K_c = 3.0$ for $m = m_1 = 0$.

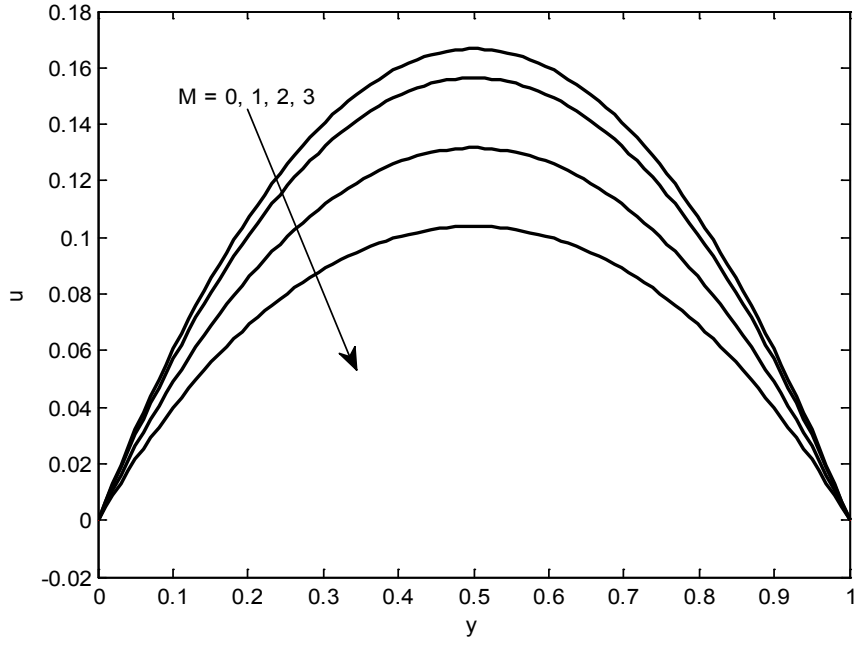

Figure 5 Velocity profiles showing the effects of *M* with $R = 0.5, S = 1.0, B = 0.5$ and $K_c = 3.0$ for $m = m_1 = 1$.

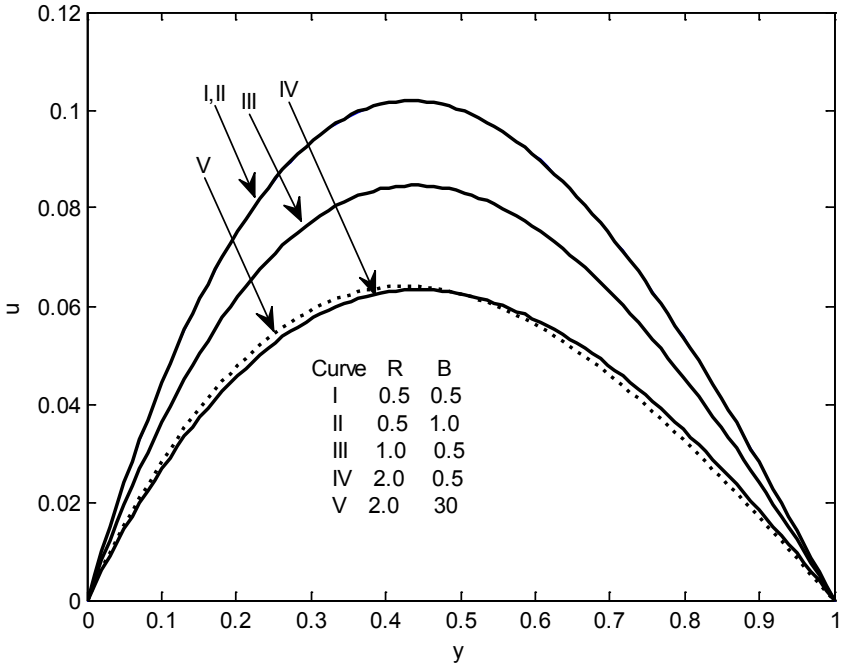

Figure 6 Velocity profiles showing the effects of *R* and *B* $(S = 0, K_c = 0)$ for M = 0 and $m = m_1 = 0$.

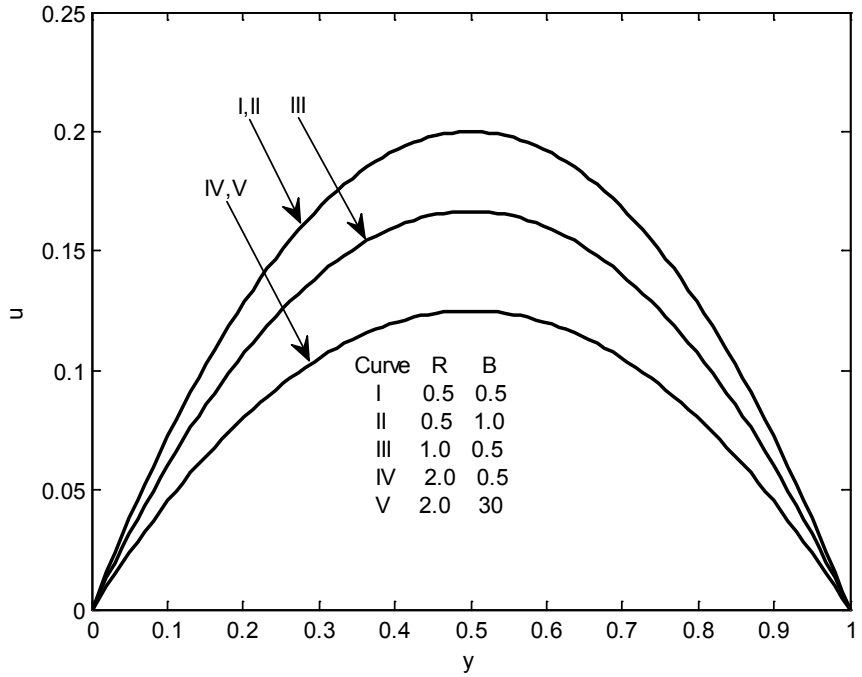

Figure 7 Velocity profiles showing the effects of *R* and *B* $(S = 0, K_c = 0)$ for M = 0 and $m = m_1 = 1$.

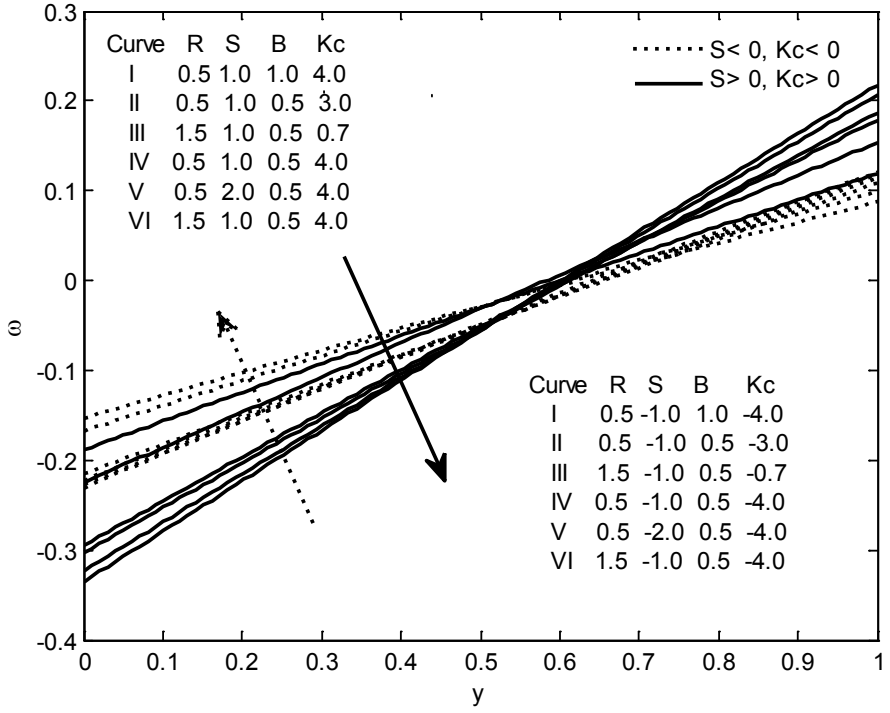

Figure 8 Micro rotation profiles showing the effects of R, S, B, K_c for M = 0 and $m = m_1 = 0$.

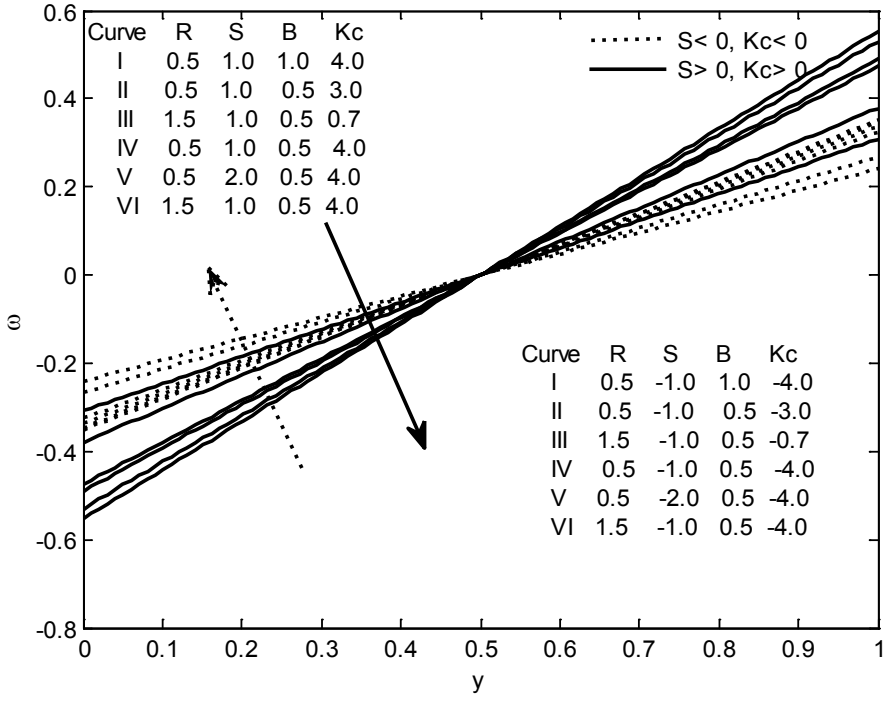

Figure 9 Micro rotation profiles showing the effects of R, S, B, K_c for M = 0 and $m = m_1 = 1$.

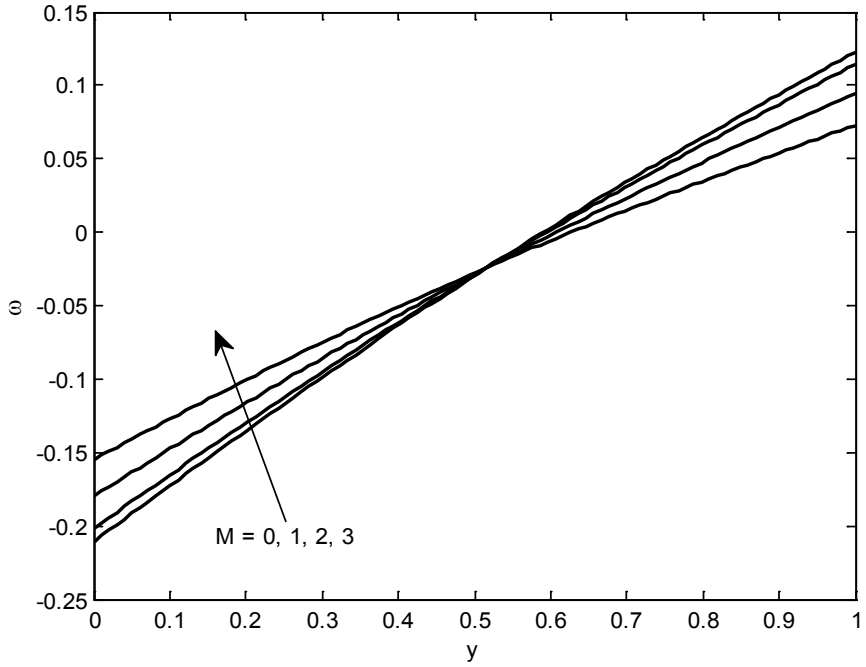

Figure 10 Microrotation profiles showing the effects of M with R = 0.5, S = 1.0, B = 0.5 and Kc = 3.0 for $m = m_1 = 0$.

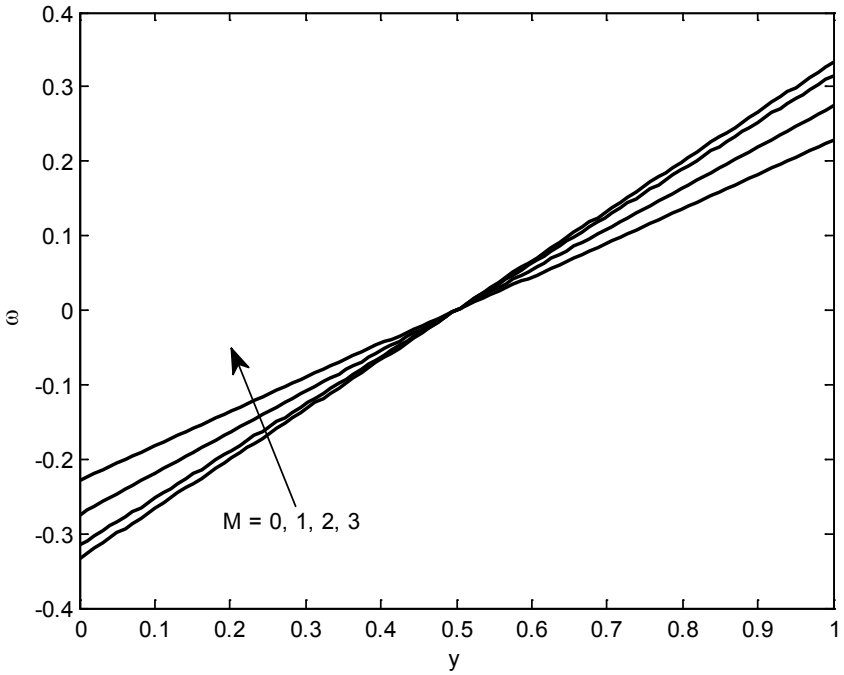

Figure 11 Microrotation profiles showing the effects of M with R = 0.5, S = 1.0, B = 0.5 and K_c = 3.0 for $m = m_1 = 1$.

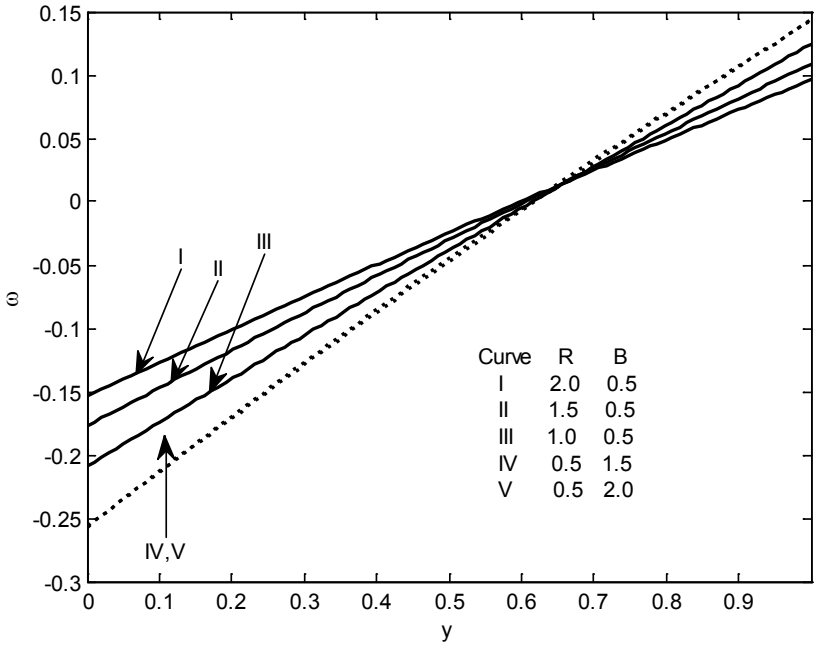

Figure 12 Micro rotation profiles showing the effects of R and B $(S=0, K_c=0)$ for M = 0 and $m=m_1=0$.

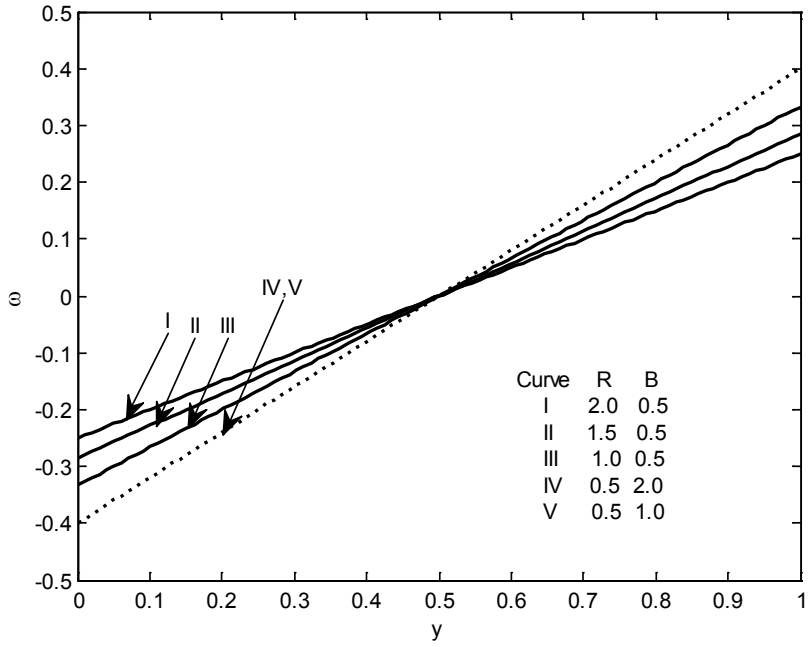

Figure 13 Micro rotation profiles showing the effects of R and B $(S=0, K_c=0)$ for M = 0 and $m=m_1=1$.

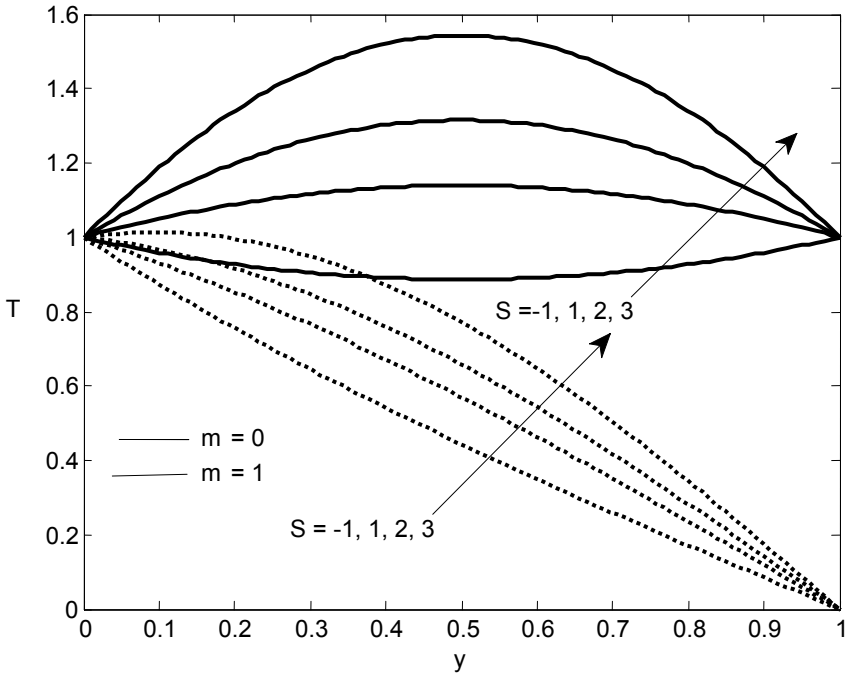

Figure 14 Temperature profiles for different values of *S* for $m = 0$ and $m = 1$.

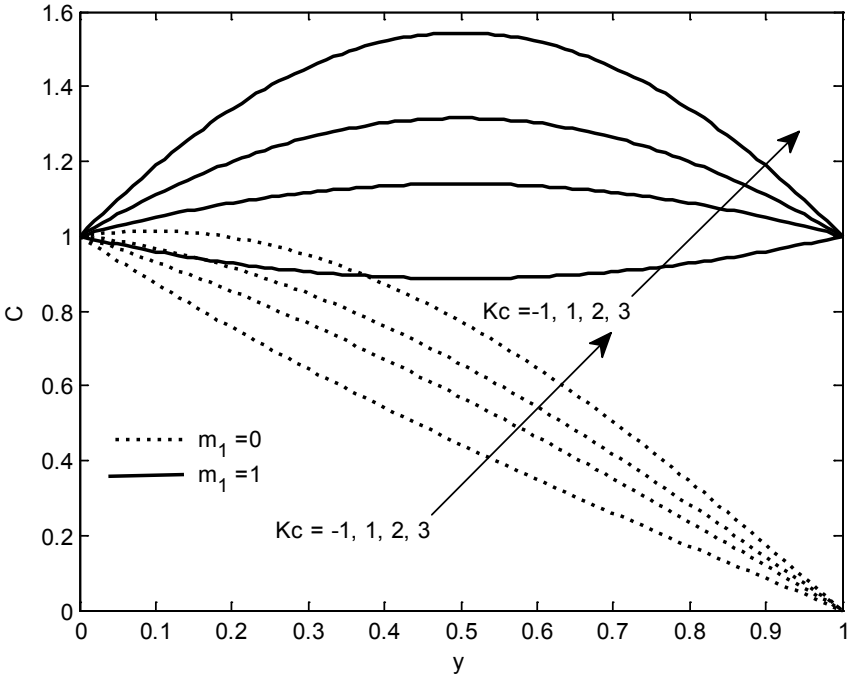

Figure 15 Concentration profiles for different values of *S* for $m_1 = 0$ and $m_1 = 1$.

Conclusion

1) The present study brings to its fold the results of previous studies in particular cases.

2) The presence of a heat source and exothermic reaction enhances the velocity at all points overriding the effects of vortex viscosity and material property in both symmetric and asymmetric cases.

3) The vortex viscosity parameter has a dominating effect attributing micropolar properties.

4) The vortex viscosity has a retarding effect on the fluid velocity.

5) Micro-rotation remains unaffected by the controlling parameters of the flow phenomena in the middle layers of the channels as the middle layers experience two mutual opposite rotations.

6) A resistive force of electromagnetic origin (Lorentz force) produced by the interaction of the current and applied magnetic field due to conducting micropolar fluid resists the velocity at all points of the channel and also resists the microrotation in the right half of the channel with an increasing magnetic parameter (M). Thus the observation is compatible as reported earlier by Cramer and Pai [25].

References

[1] AC Eringen. Theory of micropolar fluids. *J. Math. Mech*. 1966; **16**, 1-18.
[2] MM Rahman, IA Eltayeb and SMM Rahman. Thermo-micropolar fluid flow along a vertical permeable plate with uniform surface heat flux in the presence of heat generation. *Therm. Sci.* 2009; **13**, 23-36.
[3] MM Rahman. Convective flows of micropolar fluids from radiative isothermal porous surfaces with viscous dissipation and joule heating. *Comm. Nonlinear Sci. Numer. Simulat*. 2009; **14**, 3018-30.
[4] MM Rahman and T Sultana. Radiative heat transfer flow of micropolar fluid with variable heat flux in a porous medium. *Nonlinear Anal. Model. Control* 2008; **13**, 71-87.
[5] MM Rahman and T Sultana. Transient convective flow of micropolar fluid past a continuously moving vertical porous plate in the presence of radiation. *Int. J. Appl. Mech. Eng*. 2007; **12**, 497-513.
[6] MM Rahman and MA Sattar. MHD convective flow of a micropolar fluid past a continuously moving vertical porous plate in the presence of heat generation/absorption. *ASME J. Heat Tran*. 2006; **128**, 142-52.
[7] IA Hassanien, AH Essawy and NM Moursy. Natural convection flow of micropolar fluid from a permeable uniform heat flux surface in porous medium. *Appl. Math. Comput*. 2004; **152**, 323-35.
[8] O Abdulaziz and I Hashim. Fully developed free convection heat and mass transfer of a micropolar fluid between porous vertical plates. *Numer. Heat Tran. A: Appl*. 2009; **55**, 270-88.
[9] A Desseaux and NA Kelson. Flow of a micropolar fluid bounded by a stretching sheet. *ANZIAM J*. 2000; **42**, C536-C560.
[10] N Mitarai, H Hayakawa and H Nakanishi. Collisional granular flow as a micropolar fluid. *Phys. Rev. Lett.* 2002; **88**, 174301-4.
[11] HAM El-Arabawy. Effect of suction/injection on the flow of a micropolar fluid past a continuously moving plate in the presence of radiation. *Int. J. Heat Mass Tran*. 2003; **46**, 1471-7.
[12] O Aydin and I Pop. Natural convection from a discrete heated enclosure filled with micropolar fluid. *Int. J. Eng. Sci*. 2005; **43**, 1409-18.
[13] O Aydin and I Pop. Natural convection in differentially heated enclosure filled with a micropolar fluid. *Int. J. Eng. Sci.* 2007; **46**, 963-9.
[14] RA Damseh, TAA Azab, BA Shannak and MA Husein. Unsteady natural convection heat transfer of micropolar fluid over a vertical surface with constant heat flux. *Turk. J. Eng. Environ. Sci*. 2007; **31**, 225-33.
[15] AJ Chamkha, T Grosan and I Pop. Fully developed free convection of a micropolar fluid in a vertical channel. *Int. Comm. Heat Tran*. 2002; **29**, 1021-96.
[16] SK Parida, M Acharya, GC Dash and S Panda. MHD heat and mass transfer in a rotating system with periodic suction. *Arab. J. Sci. Eng*. 2011; **36**, 1139-51.

[17] J Zueco, S Ahmed and LM López-Ochoa. Magneto-micropolar flow over a stretching surface embedded in a Darcian porous medium by the numerical network method. *Arab. J. Sci. Eng.* 2014; **39**, 5141-51.
[18] NT Eldabe and MY Abou-Zeid. Magnetohydrodynamic peristaltic flow with heat and mass transfer of micropolar biviscosity fluid through a porous medium between two co-axial tubes. *Arab. J. Sci. Eng.* 2014; **39**, 5045-62.
[19] M Kar, SN Sahoo, PK Rath and GC Dash. Heat and mass transfer effects on a dissipative and radiative visco-elastic MHD flow over a stretching porous sheet. *Arab. J. Sci. Eng*., 2014; **39**, 3393-401.
[20] KA Helmy, HF Idriss and SE Kassem. MHD free convection flow of a micropolar fluid past a vertical porous plate. *Can. J. Phys*. 2002; **80**, 1661-73.
[21] M Acharya, GC Dash and LP Singh. Magnetic field effects on the free convection and mass transfer flow through porous medium with constant suction and constant heat flux. *Indian J. Pure Appl. Math*. 2000; **31**, 1-18.
[22] FP Foraboschi and ID Federico. Heat transfer in laminar flow of non-Newtonian heat-generating fluids. *Int. J. Heat Mass Tran.* 1964; **7**, 315-8.
[23] R Muthucumaraswamy. Effects of a chemical reaction on a moving isothermal vertical surface with suction. *Acta Mech*. 2002; **155**, 65-70.
[24] AA Afify. MHD free convective flow and mass transfer over a stretching sheet with chemical reaction. *Heat Mass Tran*. 2004; **40**, 495-500.
[25] KR Cramer and SI Pai. *Magnetofluid Dynamics for Engineers and Applied Physics*. Script Publishing Company, Washington DC, 1973, p. 1-144.
[26] SI Pai. *Viscous Flow Theory I - Laminar Flow*. D. Van Nostrand Company, 1956, p. 1-223.
[27] SK Ravi, AK Singh and KA Alawadhi. Effect of temperature dependent heat source/sink on free convective flow of a micropolar fluid between two vertical walls. *Int. J. Energ. Tech*. 2011; **3**, 1-8.